Electroanalysis of ascorbic acid (vitamin C) using nano-ZnO/poly(luminol) hybrid film modified electrode

S. Ashok Kumar, Hui-Wen Cheng, Shen-Ming Chen *

Department of Chemical Engineering and Biotechnology, National Taipei University of Technology, No. 1, Section 3, Chung-Hsiao East Road, Taipei 106, Taiwan, ROC

ABSTRACT

Electrochemical analysis of ascorbic acid (AsA) in physiological condition using a new hybrid film modified electrode is described. Electrochemical polymerization of luminol in 0.1 M H_2SO_4 solution was carried out using ZnO nanoparticles (ZnO-NPs) coated glassy carbon electrode (GCE) as working electrode. This hybrid film coated electrode noted as poly(luminol)/ZnO-NPs hybrid film modified GCE (PLu/ZnO-NPs/GCE). The atomic force microscope (AFM) and scanning electron microscope (SEM) studies were demonstrated that PLu/ZnO-NPs hybrid film covered the electrode surface and the ZnO-NPs particle sizes were <100 nm. The visible blue colored organic–inorganic (PLu/ZnO-NPs) hybrid films were observed on the electrode surface. Electrochemical studies proved that PLu/ZnO-NPs hybrid film modified electrode is electroactive in the pH range from 1 to 11 and the poly(luminol) (PLu) redox peak was pH dependent with a slope of -53 mV/pH. The PLu/ZnO-NPs modified electrodes electroactivity also investigated by catalyzing the oxidation of AsA, demonstrating its great potential applications in electroanalysis of AsA. The resulting, AsA electrochemical sensor exhibited a wide linear response range (from 1×10^{-6} to 3.6×10^{-4} M, $r^2 = 0.9989$), lower detection limit (1×10^{-6} M) and fast response time (3 s) for AsA determination. Our results show that PLu/ZnO-NPs hybrid film provides a novel and efficient platform for the oxidation of AsA and realizing efficient electrocatalysis and that the materials have potential applications in the fabrication of electrochemical sensors. Analysis of commercial vitamin C samples using PLu/ZnO-NPs hybrid film modified electrode was demonstrated and the obtained results are good agreement with the labeled amount.

© 2009 Elsevier Ltd. All rights reserved.

1. Introduction

The term 'vitamin C' refers to both ascorbic acid (AsA) and dehydroascorbic acid, since the latter oxidation product is reduced back to ascorbic acid in the body. AsA is well known for its radical-scavenging capacity and is the most effective water-soluble antioxidant in human plasma. It is the terminal small molecule antioxidant in many biological systems and probably the most abundant free radical scavenger in many cell types. In addition to its role as an antioxidant, the moderately positive standard redox potential of the ascorbate/monodehydroascorbate couple makes ascorbate an excellent one-electron donor to a large variety of enzymes, in particular, oxygenases and hydroxylases [1]. Fresh fruits (especially citrus fruits and black currant) and green vegetables constitute rich sources of AsA. Human milk provides enough AsA to prevent scurvy in breast-fed infants. AsA (L-*threo*-hex-2-enono-1,4-lactone) is a diacid (pK_1 = 4.2 and pK_2 = 11.8), which exists almost exclusively as the monoanion at physiological pH values [1,2].

Due to the importance of AsA in life cycle, its determination in aqueous solution is very important. Traditional procedures for AsA determination are generally based on enzymatic methods [3], on titration with oxidizing agents, like iodine or 2,6-dichlorophenolindophenol [4] and HPLC analysis with fluorimetric [4] or UV–vis detection [5,6]. Recently there is a considerable interest to develop chemical sensors for electrochemical detection of AsA. AsA can be easily oxidized electrochemically at conventional electrodes which have been used to detect AsA [7–15]. However, direct oxidation of AsA at bare electrode results in adsorption of the oxidized product on the electrode surface; it causes electrode fouling and unstable electrode response [11–15]. In addition, some of biological molecules, e.g. dopamine and uric acid undergo oxidation within same potential window as AsA. To ignore these problems, modified electrodes have been developed and reported for detection of AsA with various functional groups at lower oxidation potential [16–23].

Nanocomposites made of inorganic materials and redox polymers are possessing good mechanical strength, thermal and chemical stability. In addition to those applications, many recent efforts have centered on the design of other types of hybrid materials

---

* Corresponding author. Tel.: +886 2 27017147; fax: +886 2 27025238.
  E-mail addresses: sakumar80@gmail.com (S.A. Kumar), smchen78@ms15.hinet.net (S.-M. Chen).

which explore in various fields, for example: electrocatalysis, transducers, biomaterials, etc [24]. The embedding of inorganic nanoparticles into polymers represents a simple way to protect nanoparticles from agglomeration and take advantage of their physical characteristics [25]. Hybrid nanocomposite systems based on the nanoscaled dispersion of an inorganic phase in a thermally stable polymer matrix have attracted extensive research interest in recent years [26–30].

Zinc oxide (ZnO) has a broad range of applications, e.g. in pigments, rubber additives, gas sensors, varistors and transducers. ZnO-NPs are increasingly being used as pigments and UV absorbers in personal care products, coatings and paints, predominantly because of their UV absorbance efficiency and transparency to visible light. As a wide bandgap semiconductor material with a large excitation binding energy, ZnO has been promising applications in catalytic, electrical, optoelectronic, photochemical fields and sensors [31–35]. ZnO-NPs offers several advantages over existing biosensing platforms, most notably a large surface area for greater biofunctionalization [36] and the interest has been focused towards the applications of ZnO-NPs in chemical and biosensing because of its high isoelectric point (9.5), biocompatibility and fast electron transfer kinetics [37].
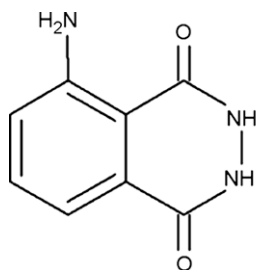
The 5-Amino-2,3-dihydro-phthalazine-1,4-dione (Luminol) (Scheme 1) has widely used in chemistry and biochemistry [38]. Furthermore, luminol has been extensively used in chemiluminescence detection [39–41] and electrochemiluminescence [42–45]. An amino group in luminol serves as electron-donating group due to its positive mesomeric effect and enhances the chemiluminescence intensity resulting from reactions on the hydrazide group.

In the present paper, a new hybrid material (PLu/ZnO-NPs) coated electrodes preparation; characterization and its potential application in electrocatalysis of AsA were reported. PLu/ZnO-NPs hybrid film was characterized using atomic force microscope (AFM) and scanning electron microscope (SEM). Cyclic voltammetry and electrochemical impedance spectroscopy (EIS) have been used to investigate the electrochemical properties. To the best of our knowledge, for the first time, PLu/ZnO-NPs hybrid film coated electrode has been used for electroanalysis of AsA in physiological condition. In addition, analysis of commercial vitamin C tablets was investigated using the proposed method.

2. Experimental

2.1. Apparatus

Electrochemical measurements were performed with CH Instruments (TX, USA) Model-400 potentiostat with a conventional three-electrode cell. A BAS GCE or ZnO-NPs/GCE was employed as working electrodes. Platinum wire is used as auxiliary electrode. All the cell potentials were measured with respect to an Ag/AgCl [KCl (sat)] reference electrode. Amperometric studies were performed on a Bi-potentiostat Model CHI750A (TX, USA) having an analytical rotator model AFMSRK with MSRX speed control (PINE Instruments, USA). Hitachi scientific instruments (London, UK) Model S-3000H scanning electron microscope was used for surface image measurements. The AFM images were recorded with a multimode scanning probe microscope system operated in tapping mode using model CSPM4000 Instruments, Ben Yuan Ltd. (Beijing, China). Electrochemical impedance measurements were performed using an impedance measurement unit, IM6ex ZAHNER, Messsysteme (Kroanch, Germany). All the pH measurements were performed on Suntex Model SP-701 pH meter (Jiangsu, China). All the experiments were carried out at an ambient room temperature of 25 ± 2 °C.

2.2. Reagents

All chemicals were of analytical reagent grade unless otherwise specified. Luminol was purchased from Aldrich (Milwaukee WI, USA) and used as received. Dopamine hydrochloride, uric acid and ZnO-NPs (<100 nm) were purchased from Sigma–Aldrich (St. Louis, MO, USA). Sulfuric acid and sodium hydroxide were purchased from Wako pure chemicals (Osaka, Japan). Ascorbic acid, sodium acetate and sodium dihydrogen phosphate were received from E-Merck (Darmstadt, Germany) and used without further purification. Water was obtained from a Millipore Alpha-Q Lotun ultrapure water system (18 MΩ resistivity). Solutions and buffers were prepared employing standard laboratory procedures. Before each experiment the solutions were deoxygenated by purging with pre-purified nitrogen gas. Vitamin C tablets were purchased from a local drug store in Taipei.

2.3. Modified electrode preparation

ZnO-NPs suspension was prepared by dissolving 10 mg of accurately weighed ZnO-NPs in 10 ml dimethyl formamide and then ultrasonicated for 10 min to create a homogenous suspension. Prior to the electrode modification, the GCE was mechanically polished with alumina powder (Al$_2$O$_3$, 0.05 μ) up to a mirror finish and ultrasonicated in distilled water for 5 min. Then GCE was electrochemically activated by using 10-times cyclic potential sweeps in the range from −0.5 to 1.0 V in 0.1 M H$_2$SO$_4$ solution at a scan rate of 0.1 Vs^{-1}. The mixture of 10 μl ZnO-NPs suspension was spread evenly onto the surface of pretreated GCE which was dried for 3 h in the absence of light; the solvents evaporated and left the ZnO-NPs on the electrode surface. Finally, the ZnO-NPs modified electrode was thoroughly rinsed with double-distilled water. Thereafter, ZnO-NPs/GCE electrode was cycled in 0.1 M H$_2$SO$_4$ solution containing 0.5 mM luminol between the potential ranges from 0.0 to 1.0 V for 20 cycles. Afterwards, the electrode was thoroughly rinsed with double-distilled water and then dried at room temperature for an hour in the absences of light. When not in use, the electrode was stored in aqueous solution of 0.1 M phosphate buffer solution (PBS, pH 7.0) at 4 °C. It was noted as PLu/ZnO-NPs/GCE and then used for further studies. For comparison, ZnO-NPs/GCE and PLu/GCE were prepared and used for further investigation.

3. Results and discussion

3.1. Electrochemical polymerization of luminol

Fig. 1 shows consecutive cyclic voltammograms (CVs) of luminol polymerization on ZnO-NPs modified GCE from 0.1 M H$_2$SO$_4$ solution containing 0.5 mM luminol. On the first anodic scan an oxidation peak was observed at +0.93 (Pa$_1$) which is corresponding

Scheme 1. Chemical structural formula of luminol.
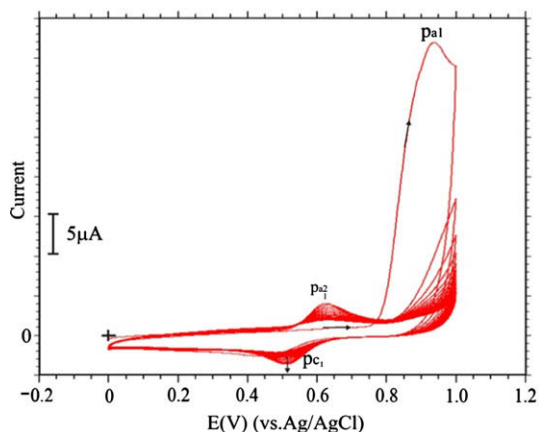
Fig. 1. CVs of the PLu film growth on ZnO-NPs coated GCE from the electrolyte 0.1 M H_2SO_4 solution containing 5×10^{-4} M luminol monomers. Scan rate = 0.05 V/s.

to the oxidation of a primary amino group of luminol monomers [46–51]. Upon scan reversal a cathodic wave with a peak potential centered at 0.49 V (Pc_1) was observed. On the second and subsequent potential scans, an additional anodic peak was observed at +0.62 V (Pa_2) with the potential cycle repeating, the peaks start to appear and grow. This behavior is attributed to the deposition and growth of an electroactive layer on the electrode surface. At the same time, it was also observed that polymer film growth was faster for the first twenty cycles than other subsequent cycles. From the 19th cycle on, the film hardly grew, which indicated that polymerization reached saturation. After electropolymerization, a uniform adherent dark blue polymer observed on the GCE surface. According to the literature reports [50–53], it was the intermolecular $–NH_2$ functional group monomers were involved in the polymerization reaction. The oxidation of luminol via NH_2 moiety leads to dimerization, ultimately to the formation of polymer through a progressively more facile oxidation of the dimer, trimer, tetramer, etc. and the consequent coupling and deprotonation. The chemical composition of poly(luminol) film is possibly analogous to that of polyaniline (PANI). PANI has been confirmed to exist in the form of a sequence of benzene rings, alternating in reduced and oxidized segments, or as only oxidized dimeric segments [46–51]. The redox reaction of PLu is analogous to the fully redox form of polyaniline that is shown in Scheme 2.

### 3.2. SEM, AFM and EIS studies

SEM (a and b) and AFM images (c and d) of ZnO-NPs (a and c) and PLu/ZnO-NPs (b and d) coated electrodes are shown in Fig. 2. As seen in SEM and AFM images, ZnO-NPs are covered the electrode surface and the size of particles were <100 nm (a and c). Fig. 2b and d shows the surface morphology of PLu/ZnO-NPs hybrid

film coated electrode. These topography images confirmed that ZnO-NPs were embedded in the PLu film matrix. Using AFM software image analyzer, the approximate thickness of the ZnO-NPs film and PLu/ZnO-NPs film coated electrodes were predicted as 77 and 435 nm, respectively (Fig. 2c and d).

Fig. 3 exhibits the electrochemical impedance spectroscopy of differently modified electrodes. EIS has been used for studying the interface properties of surface-modified electrodes. The typical impedance spectrum includes a semicircle portion at higher frequencies corresponding to the electron transfer limited process and a linear part at a lower frequency range representing the diffusion limited process. The semicircle diameter in the impedance spectrum equals the electron transfer resistance, R_{ct}. The respective semicircle diameter corresponds to the electron transfer resistance at the electrode surface [54,55]. Fig. 3A and B show the complex plane diagram (Z' vs. Z'', Nyquist plot) of the EIS measurement of PLu/ZnO-NPs/GCE (curve a), PLu/GCE (curve b), ZnO-NPs/GCE (curve c), and bare GCE (curve d) in the presence of equivalent 5 mM $[Fe(CN)_6]^{3-/4-}$ + 0.1 M KCl. It can be seen at the bare GCE (Fig. 3B curve d), a small semicircle of about 80 Ω diameter with an almost straight tail line present. This is indicative of the characteristic of a diffusion-controlled electrode process [54,55]. A semicircular Nyquist impedance spectrum is observed for ZnO-NPs/GCE, this phenomenon indicates that the electron transfer resistance at the electrode/electrolyte interface increases after surface modification with ZnO-NPs. However, PLu/GCE (curve b) and PLu/ZnO-NPs/GCE (cuve a) Nyquist plots show a linear part at higher frequency, thus confirming that after the modification of PLu and PLu/ZnO-NPs films, the electrode process is a diffusion controlled. However, a linear part at higher frequency for PLu and PLu/ZnO-NPs film, suggesting that a significant acceleration of the $[Fe(CN)_6]^{3-/4-}$ redox reaction occurred due to the presence of polymer and ZnO-NPs. The decreasing of charge transfer resistance value for PLu/ZnO-NPs/GCE is because of polymer and ZnO-NPs can act as an electron transfer medium and enhanced electron transfer and also indicated that hybrid film had been attached to the electrode surface [54–56].

3.3. Electrochemical properties

A PLu/ZnO-NPs modified electrode was transferred into a test buffer solution to investigate the electroactivity using cyclic voltammetry. The PLu/ZnO-NPs/GCE showed a pair of redox peaks in various pH buffer solutions (1–11). The dependence of the redox processes on pH was observed (Fig. S1). It was clear that the magnitude and the position of the redox peak depend on pH. As pH increases, the magnitude of the peak slowly diminishes and the peak potential, E_p, shifts to less anodic values. The decrease in redox peak currents (i_p) were observed with the increase of pH indicates that the kinetics of the oxidation and reduction processes depend on the concentration of H^+ ions in the solution. In other words, the transport of protons is involved in the rate-determining step of the redox processes.
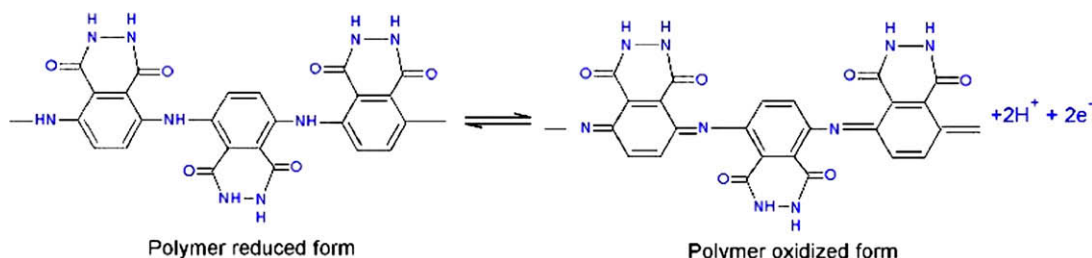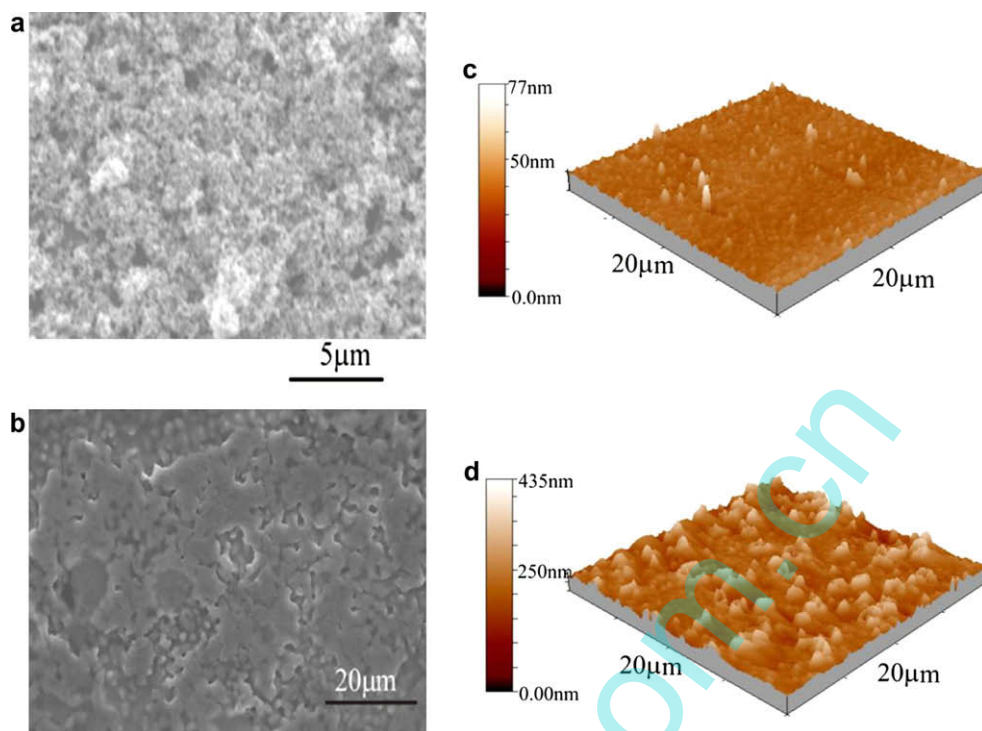

Scheme 2. Redox reaction of Poly(luminol).

Fig. 2. SEM (a and b) and AFM (c and d) images of ZnO-NPs film and PLu/ZnO-NPs hybrid film modified electrodes.

The format potential ($E^{0'} = E_{pa} + E_{pc}/2$) decreases linearly with respect to the pH of the buffer solution with a slope of −53 mV/pH. This indicates that the electroactivity of PLu involves equal number of proton/electron elimination/addition in the oxidation/reduction processes (Scheme 2). The electroactivity of polyaromatic amines requires the presence of protons in the medium, where electrons and protons must be exchanged during the redox processes with switching in conductivity of the polymer [46–52]. This situation is usually met in the examination of the electroactivity of aromatic amine-based conducting polymers such as poly(p-aminobenzene sulfonic acid), PANI, etc [19,22,46–53].

An $E^{0'}$ for the redox processes of PLu/ZnO-NPs modified electrode in acidic solution (pH 1.0) was estimated as 0.51 V vs. Ag/AgCl. The effect of scan rate on the redox peak currents of PLu films in 0.1 M H₂SO₄ solution was investigated (Fig. S2). It is clear that the peak current increases as the scan rate, v, increases, while the peak potential is practically insensitive to the change in v and the peak separation (ΔE_p) was nearly 0.07 V within the tested v range

Fig. 3. EIS obtained for PLu/ZnO-NPs/GCE (curve a), PLu/GCE (curve b) and ZnO-NPs/GCE (curve c) and bare GCE (curve d) in 5 mM [Fe(CN)₆]³⁻/⁴⁻ + 0.1 M KCl solutions by applying an AC voltage with 5 mV amplitude in a frequency range from 100 MHz to 100 kHz.

(10–500 mV/s). This indicates that the electroactivity of PLu film is similar to that of surface-attached electroactive sites [57]. The surface coverage (Γ) calculated by integration of the charge under the anodic voltammetric wave for PLu/GCE and PLu/ZnO-NPs/GCE. According to the equation, $Q = nFA\Gamma$ where n is the number of electrons, A is the working electrode area (0.0707 cm²), v scan rate and other parameters have their usual meanings [57], the surface coverage's were calculated as 3.228×10^{-10} mol/cm² (PLu/ZnO-NPs/GCE) and 1.238×10^{-10} mol/cm² (PLu/GCE). PLu/ZnO-NPs modified electrode shows higher peak current than PLu modified electrode which indicated that ZnO-NPs increased the surface area of the modified electrode (Fig. S3).

The stability of PLu/ZnO-NPs/GCE and PLu/GCE modified electrodes were evaluated by cycling 100× in the potential range between 0.3 and 0.7 V in 0.1 M H₂SO₄ solution at a scan rate of 100 mVs⁻¹. It was observed that redox peak current of PLu/ZnO-NPs modified electrode remained stable on continuous cycling even more than 100 cycles. However, redox response of PLu modified electrode was gradually decreased (20% after 100 cycles). Good stability of the PLu/ZnO-NPs hybrid film may reflect the irreversible deposition and strong adherent of PLu/ZnO-NPs on the electrode surface. Recent studies were confirmed that existence of interaction between ZnO-NPs and polyaniline (PANI) molecular chain [58,59]. Further, there result indicates the interaction between the ZnO particles and PANI molecular chains due to the adsorption of PANI molecular chains on the surface of the ZnO particles. Since the polymer structure of PLu was similar to PANI, similar interactions might be involved between ZnO-NPs and PLu hybrid film. However, further studies are required to evaluate the existing interaction between the ZnO-NPs and PLu film.
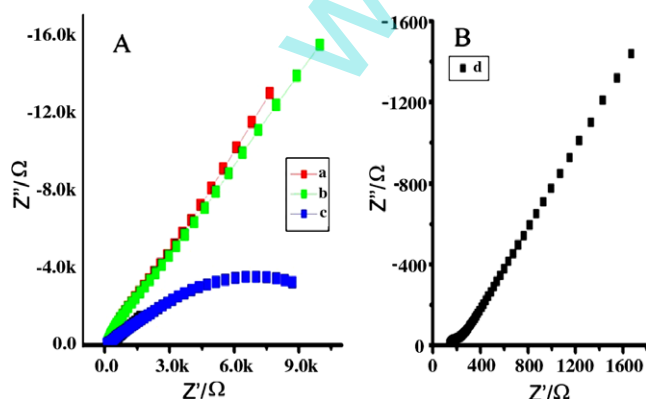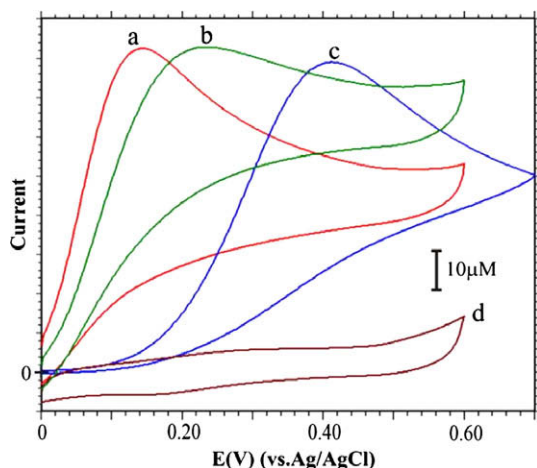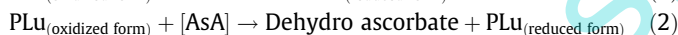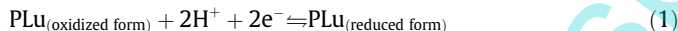
3.4. Electrocatalytic oxidation of ascorbic acid

The CVs were recorded at 40 mVs⁻¹ using PLu/ZnO-NPs/GCE (curve a), PLu/GCE (curve b), bare GCE (curve c) in pH 7.0 phosphate buffer solution (PBS) with 5 mM AsA as shown in Fig. 4. Fig. 4 curve d shows the CVs of PLu/ZnO-NPs modified electrode

Fig. 4. CVs of PLu/ZnO-NPs/GCE (curve a), PLu/GCE (curve b) and bare GCE (curve c) in pH 7.0 PBS + 5 mM AsA. A PLu/ZnO-NPs/GCE in the absences of AsA in PBS (pH 7.0) solution (curve d). Scan rate = 10 mV/s.

in the absence of AsA in 0.1 M PBS. The greatly enhanced oxidation current in the presence of AsA at 0.1 V shows that PLu/ZnO-NPs hybrid film could catalyze the oxidation of AsA effectively. It was obvious that AsA diffuses to the electrode surface and reacts with the hybrid films of PLu/ZnO-NPs. Thus, a large increase of anodic current was observed which is resulting from the electrocatalytic oxidation of AsA on hybrid film modified electrode (Fig. 4 curve a). In comparison with the results obtained at a bare GCE, in which the potential for the oxidation of AsA was observed at 0.41 V. The PLu/ZnO-NPs hybrid film lowered the anodic overpotential of AsA by about 280 mV. The electrocatalytic oxidation of AsA at PLu/ZnO-NPs modified electrode could be explained as follows (Eqs. (1) and (2)) [46–48].

$$PLu_{(oxidized\ form)} + 2H^+ + 2e^- \leftrightharpoons PLu_{(reduced\ form)} \qquad (1)$$
$$PLu_{(oxidized\ form)} + [AsA] \rightarrow Dehydro\ ascorbate + PLu_{(reduced\ form)} \qquad (2)$$

Its worth to compare AsA response at PLu/GCE (curve b) and PLu/ZnO-NPs/GCE (curve a) modified electrodes. The oxidation potential of AsA at PLu/GCE was 0.236 V which was higher than potential observed (0.10 V) at PLu/ZnO-NPs/GCE. This result reflects the synergistic effect of PLu/ZnO-NPs hybrid films and showed the applications of hybrid film modified electrode. This behavior can be explained based on pK_a of AsA (pK_{a1} 4.04 and pK_{a2} 11.34) [1,2], in neutral condition AsA exist as a monodeprotonated ascorbate anion so it may have affinity towards positively charged ZnO-NPs. In addition, the improvement of the electrocatalytic activity observed in the presence of ZnO-NPs is likely due to their positive charge that may facilitate the access of AsA (in the anionic form at pH7) to the electrode surface.

3.5. Effect of scan rate and pH

The dependence of oxidation peak currents of AsA on the scan rate was studied (Fig. S4). It was observed that the peak current (i_p) increased with scan rate ($v^{1/2}$) from 0.01 to 0.20 V/s. According to the i_p–$v^{1/2}$ curve, the current increased linearly with the square root of the scan rate, from which we deduced that the electrode reaction was diffusion controlled.

Varying the pH of the supporting electrolyte would bring on different current responses of AsA. The effects of the medium pH on the oxidation peak current of AsA using PLu/ZnO-NPs/GCE were investigated. The oxidation currents which were dependent on the pH value of buffer solution showed that AsA oxidation reaction
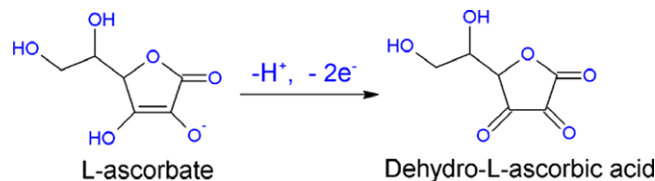

Scheme 3. Electrocatalytic oxidation of AsA on PLu/ZnO-NPs hybrid film.

includes some proton transfer processes (Fig. S5a). The oxidation of L-ascorbate to dehydro-L-ascorbic acid (Scheme 3) involves the transfer of two electrons and one proton [16,46]. It was proposed that the oxidation of ascorbate on the poly(aniline)-poly(vinylsulfonate) composite film occurs through an analogous kinetic mechanism in which a complex is formed between the polymer and the ascorbate and that this is followed by oxidation of bound ascorbate [60]. Since PLu structure is analogous to PANI, electrochemical oxidation of ascorbate on PLu film might follow similar oxidation processes. However, further studies are required to unravel the electrocatalytic processes of ascorbate on PLu/ZnO-NPs hybrid film. In the range of pH 1–11, the anodic peak current of AsA is influenced and the catalytic current dramatically increases up to pH 7.0 and then started to decrease in higher pH value (Fig. S5b). For this reason, the physiological pH 7.0 has been selected for further investigation of AsA at PLu/ZnO-NPs hybrid film modified electrode.

3.6. Amperometric determination of ascorbic acid

Analytical performance of hybrid film modified electrode for AsA detection was investigated. Fig. 5 shows the amperometric responses of PLu/ZnO-NPs hybrid film modified electrode for AsA detection at an applied potential of 0.1 V. The hybrid film modified electrode displays rapid and good linear response. The PLu/ZnO-NPs hybrid film modified electrode showed linear response for AsA determination from 1×10^{-6} to 3.6×10^{-4} M with a correlation coefficient of 0.9989. The response time was 3 s when the current reached 95% of the steady state. The detection limit was found to be 1×10^{-6} M on signal-to-noise ratio of 3.

The lowest detection limit, linear range and lower working potential (0.1 V at pH 7.0) of the proposed method are considerable and comparable with some of known AsA sensors [16–23,61–65].
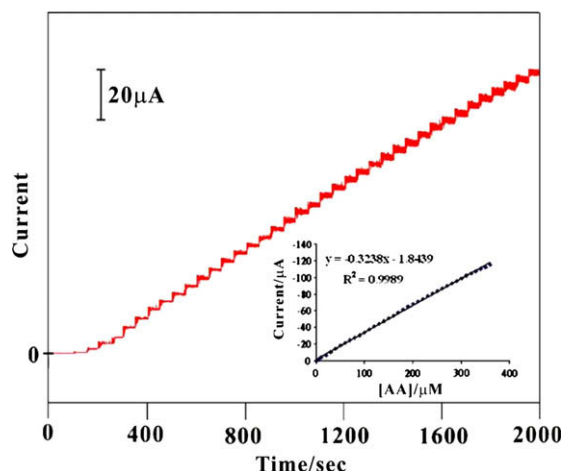
Fig. 5. The amperometric responses recorded using PLu/ZnO-NPs/GCE at an applied potential of 0.1 V vs. Ag/AgCl to successive addition of 1×10^{-6}–3.6×10^{-4} M AsA in 0.1 M PBS (pH 7.0), rotation rate = 1000 rpm. The inset figure shows the calibration plot.

The lower working potential and lower detection limit may attribute to the superior transducing ability of PLu/ZnO-NPs hybrid film modified electrode. As shown in Fig. 4, (curve a) oxidation of AsA observed at lower potential (0.1 V) on hybrid film (PLu/ZnO-NPs) modified electrode. In contrast, AsA oxidation potential was 0.236 on PLu modified electrode (Fig. 4, curve b). From these observations, we could say that synergistic effect of ZnO-NPs with PLu is preferable for the AsA detection and improves the performances of the modified electrode.

3.7. Interferences on analytical response

The typical interfering species such as dopamine and uric acid was investigated through adding 10 mM dopamine and 10 mM uric acid into pH 7.0 PBS using PLu/ZnO-NPs hybrid film modified electrode at 0.1 V. Uric acids did not produce any observable signal on the modified electrode. However, the addition of dopamine increased 2% peak currents. But, further addition of 5 mM AsA into the same buffer solution results oxidation current of AsA (Fig. 6). This result clearly indicated that dopamine and uric acid are not considerable interference in the steady state current of AsA at 0.1 V. It may be attributed to the lower working potential (0.1 V) employed for the oxidation of AsA promoted by PLu/ZnO-NPs hybrid layer.

3.8. Stability, reproducibility and shelf-life

In order to study the reproducibility of the sensor and reliability of fabrication procedure, six times PLu/ZnO-NPs hybrid film modified GCE were prepared independently. CVs of sensors were recorded in 0.1 M PBS. The relative standard deviation (R.S.D.) value of measured anodic peak currents was 3.0%. The R.S.D. of the response current obtained from the six hybrid film modified electrodes to 5×10^{-3} M AsA was found to be 2.3%. For five replicate measurements of 5×10^{-3} M AsA using a typical modified electrode, the R.S.D. was 1.8%. These data represents the reproducibility of electrode fabrication procedure and good repeatability of the sensor. The storage stability (Shelf-life) of PLu/ZnO-NPs modified electrode in 0.1 M PBS (pH 7.0) at 4 °C was evaluated. A loss of 5% in the response signal was observed after first 10 days by every day use. However, 85% response current is still retained after 30 days. This implies that PLu/ZnO-NPs modified electrode is considerably stable. However, the time required for electrode preparation is less than 30 min, so it can be prepared easily for instant use.
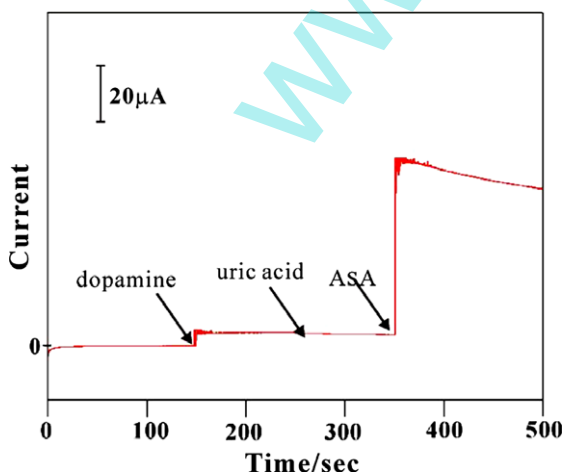
Fig. 6. Typical amperometric curve obtained with a PLu/ZnO-NPs/GCE in 0.1 M phosphate buffer solution (pH 7.0) at an applied potential of 0.1 V vs. Ag/AgCl, stirring rate = 1000 rpm. Successive additions of (a) 10 mM dopamine, (b) 10 mM uric acid, (c) 5 mM ascorbic acid.

Table 1
Determination of AsA in commercial drugs.

Samples	Labeled (mg)	Found[a] (mg)	R.S.D (%)	Recovery (%)
Tablet 1	500	492.4	2.71	98.48
Tablet 2	500	490.7	3.23	98.14

[a] Average value of three measurements.

3.9. Determination of AsA in real samples

Analytical applicability of the modified electrode was evaluated by determining the recoveries of 500 mg ascorbic acid tablet by standard addition method. A vitamin C tablet is finely powdered and accurately weighed into phosphate buffer solution; diluted samples were analyzed using PLu/ZnO-NPs/GCE modified electrode by amperometry. The obtained results are presented in Table 1. In our experiments, the concentration of AsA was calculated using standard additions method. The R.S.D of each sample for three times parallel detections is less than 3.23%. In addition, the recovered ratio based on this method was investigated and the value is between 98.48% and 98.14%. The recovered ratio indicates that determination of AsA using the proposed method is effective and can be applied for the detection of AsA in commercial samples.

4. Conclusions

A new PLu/ZnO-NPs hybrid film modified electrode was fabricated and its electrochemical properties were investigated. The electrocatalytic properties of PLu/ZnO-NPs hybrid film modified electrode towards AsA were investigated by cyclic voltammetry and amperometry. It was found that peak current responses of AsA were improved significantly and the oxidation peak shifted towards more negative potential on PLu/ZnO-NPs hybrid film modified electrode. The results indicated that the hybrid film provided a good platform for the determination of AsA at lower potential. The enhanced electrocatalytic activity of PLu/ZnO-NPs/GCE towards AsA mainly came from the combined properties of PLu/ZnO-NPs such as strong adsorptive ability and larger specific area. The hybrid film modified electrode displays linear response from 1×10^{-6} to 3.6×10^{-4} M AsA with the correlation coefficient of 0.9989. The response time was 3 s when the current reached 95% of the steady state. The detection limit was found to be 1×10^{-6} M on signal-to-noise ratio of 3. This new method can be applied for electroanalysis of ascorbic acid.

Acknowledgment

Appendix A. Supplementary data

Supplementary data associated with this article can be found, in the online version, at doi:10.1016/j.reactfunctpolym.2009.03.001.

References

[1] G.F.M. Ball, Vitamins: Their Role in the Human Body, Blackwell Publishing Professional, State Avenue, Ames, Iowa, USA, 2004, pp. 303–403.
[2] R. Banerjee (Ed.), Redox Biochemistry, John Wiley and Sons Inc., Hoboken, New Jersey, 2008, pp. 22–26.
[3] A. Marchesini, F. Montuori, D. Muffato, D. Mestri, J. Food Sci. 39 (1974) 568.
[4] R. Kirk, R. Sawyer, Pearson's Composition and Analysis of Food, ninth ed., Longman, Harlow, UK, 1991.
[5] E.S. Wagner, B. Lindley, R.D. Coffin, J. Chromatogr. 163 (1979) 225.
[6] J.W. Finley, E.J. Duang, Chromatogr. 207 (1981) 449.

[7] M. Dominguez, A. Aldaz, F. Sanchez-Burgos, J. Electroanal. Chem. 68 (1976) 345.
[8] M. Rueda, A. Aldaz, F. Sanchez-Burgos, Electrochim. Acta 23 (1978) 419.
[9] P. Karabinas, D. Jannakoudakis, J. Electroanal. Chem. 160 (1984) 159.
[10] O. Hammerich, B. Svensmark, In organic electrochemistry, in: H. Lund, M.M. Baizer (Eds.), An Introduction and a Guide, third ed., Marcel Dekker, New York, 1991 (Chapter 16).
[11] S. Lupu, A. Mucci, L. Pigani, R. Seeber, C. Zanardi, Electroanal. 14 (2002) 519.
[12] S.B. Khoo, F. Chen, Anal. Chem. 74 (2002) 5734.
[13] M.H. Pournaghi-Azar, H. Razmi-Nerbin, B. Hafezi, Electroanal. 14 (2002) 206.
[14] L. Zhang, Y.G. Sun, Anal. Sci. 17 (2001) 939.
[15] X. Lu, B. Lv, Z. Xue, M. Zhang, Y. Wang, J. Kang, Anal. Lett. 35 (2002) 1811.
[16] A. Malinauskas, R. Garjonyte, R. Mažeikiene, I. Jurevičiute, Talanta 64 (2004) 121.
[17] X. Zou, L. Luo, Y. Ding, Q. Wub, Electroanal. 19 (2007) 1840.
[18] A. Sivanesan, P. Kannan, S. Abraham John, Electrochim. Acta 52 (2007) 8118.
[19] H. Yao, Y. Sun, X. Lin, Y. Tang, L. Huang, Electrochim. Acta 52 (2007) 6165.
[20] B. Wang, T. Noguchi, J.-I. Anzai, Talanta 72 (2007) 415.
[21] T.R.L.C. Paixão, M. Bertotti, J. Pharmaceut. Biomed. 46 (2008) 528.
[22] S.A. Kumar, P.-H. Lo, S.-M. Chen, Biosens. Bioelectron. 24 (2008) 518.
[23] B.B. Prasad, S. Srivastava, K. Tiwari, P.S. Sharma, Mater. Sci. Eng. C (2008), doi:10.1016/j.msec.2008.09.025.
[24] P.M. Ajayan, L.S. Schadler, P.V. Braun, Nanocomposite Science and Technology, Wiley-VCH, Weinheim, 2003.
[25] L. Nicolais, G. Carotenuto, Metal–polymer Nanocomposites, Wiley, Hoboken, 2005.
[26] L. Francois, M. Mostafavi, J. Belloni, J.F. Delouis, J. Delaire, P. Feneyrou, J. Phys. Chem. B 104 (2000) 6133.
[27] Y. Lu, G.L. Liu, L.P. Lee, Nano Lett. 5 (2005) 5.
[28] S.A. Kumar, S.-M. Chen, Anal. Chim. Acta 592 (2007) 36.
[29] Y.P. Sun, J.E. Riggs, H.W. Rollins, R. Guduru, J. Phys. Chem. B 103 (1999) 77.
[30] J. Yang, T. Hasell, W. Wang, J. Li, P.D. Brown, M. Poliakoff, E. Lesterb, S.M. Howdle, J. Mater. Chem. 18 (2008) 998.
[31] P. Yang, H. Yan, S. Mao, R. Russo, J. Johnson, R. Saykally, N. Morris, J. Pham, R. He, H.J. Choi, Adv. Funct. Mater. 12 (2002) 323.
[32] H. Yan, R. He, J. Pham, P. Yang, Adv. Mater. 15 (2003) 402.
[33] L. Dong, J. Jiao, D.W. Tuggle, J.M. Petty, S.A. Elliff, M. Coulter, Appl. Phys. Lett. 82 (2003) 1096.
[34] Z.R. Tian, J.A. Voigt, J. Liu, B. Mckenzie, M.J. Mcdermott, M.A. Rodriguez, H. Konishi, H. Xu, Nat. Mater. 2 (2003) 821.
[35] C. Boeckler, A. Feldhoff, T. Oekermann, Adv. Funct. Mater. 17 (2007) 3864.
[36] J.W. Soares, D.M. Steeves, D. Ziegler, B.S. DeCristofano, in: Proceedings of SPIE – The International Society for Optical Engineering, Surface Modification of Nanocrystalline Zinc Oxide for Bio-sensing Applications, vol. 6370, 2006, p. 637011.
[37] S.A. Kumar, S.-M. Chen, Anal. Lett. 41 (2008) 141.
[38] J. Schiller, J. Arnhold, J. Schwinn, H. Sprinz, O. Brede, K. Arnold, Free Radical Res. 30 (1999) 45.
[39] T. Kamidate, H. Watanabe, Talanta 43 (1996) 1733.
[40] M. Fisher, S. Harbon, B.R. Rabin, Anal. Biochem. 227 (1995) 23.
[41] U. Ma, U. Jarzak, W. Thiemann, Anal. Chim. Acta 362 (1998) 121.
[42] C.E. Taylor IV., S.E. Creager, J. Electroanal. Chem. 485 (2000) 114.
[43] G. Xu, S. Dong, Anal. Chim. Acta 412 (2000) 235.
[44] O.V. Reshetnyak, E.P. Koval'chuk, Electrochim. Acta 43 (1998) 465.
[45] C.-Z. Zhao, N. Egashira, Y. Kurauchi, K. Ohga, Electrochim. Acta 43 (1998) 2167.
[46] S.-M. Chen, K.-C. Lin, J. Electroanal. Chem. 523 (2002) 93.
[47] Y.-T. Chang, K.-C. Lin, S.-M. Chen, Electrochim. Acta 51 (2005) 450.
[48] K.-C. Lin, S.-M. Chen, J. Electroanal. Chem. 589 (2006) 52.
[49] V. Ferreira, A.C. Cascalheira, L.M. Abrantes, Thin Solid Films 516 (2008) 3996.
[50] V. Ferreira, A.C. Cascalheira, L.M. Abrantes, Electrochim. Acta 53 (2008) 3803.
[51] G.-F. Zhang, H.-Y. Chen, Anal. Chim. Acta 419 (2000) 25.
[52] S.A. Kumar, S.-M. Chen, Sens. Actuators, B 123 (2007) 964.
[53] S.A. Kumar, C.-F. Tang, S.-M. Chen, Talanta 74 (2008) 860.
[54] S.A. Kumar, P.-H. Lo, S.-M. Chen, Nanotechnology 19 (2008) 255501.
[55] J. Lin, C. He, L. Zhang, S. Zhang, Anal. Biochem. 384 (2009) 30.
[56] M.D.L. Oliveira, M.T.S. Correia, L.C.B.B. Coelho, F.B. Diniz, Colloids Surface B 66 (2008) 13.
[57] A.J. Bard, L.R. Faulkner, Electrochemical Methods Fundamentals and Applications, Wiley, New York, 1980, pp. 521–525.
[58] B.K. Sharma, A.K. Gupta, N. Khare, S.K. Dhawan, H.C. Gupta, Synth. Met. (2008), doi:10.1016/j.synthmet.2008.10.010.
[59] B.K. Sharma, N. Khare, S.K. Dhawan, H.C. Gupta, J. Alloys Compd. (2008), doi:10.1016/j.jallcom.2008.10.004.
[60] P.N. Bartlett, E.N.K. Wallace, Phys. Chem. Chem. Phys. 3 (2001) 1491.
[61] C.-F. Tang, S.A. Kumar, S.-M. Chen, Anal. Biochem. 380 (2008) 174.
[62] I. Jurevičiutė, K. Brazdžiuvienė, L. Bernotaitė, B. Šalkus, A. Malinauskas, Sens. Actuators, B 107 (2005) 716.
[63] W.Z. Zhang, X.-W. Kan, S.-F. Jiao, J.-G. Sun, D.-S. Yang, B. Fang, J. Appl. Polymer Sci. 102 (2006) 5633.
[64] L. Zhang, Electrochim. Acta 52 (2007) 6969.
[65] L. Zhang, C. Zhang, J. Lian, Biosens. Bioelectron. 24 (2008) 690.